Particle creation by a moving boundary with a Robin boundary condition

2006 J. Phys. A: Math. Gen. 39 11325

(http://iopscience.iop.org/0305-4470/39/36/013)

INSTITUTE OF PHYSICS PUBLISHING JOURNAL OF PHYSICS A: MATHEMATICAL AND GENERAL

J. Phys. A: Math. Gen. **39** (2006) 11325–11333 doi:10.1088/0305-4470/39/36/013

Particle creation by a moving boundary with a Robin boundary condition

B Mintz, C Farina, P A Maia Neto and R B Rodrigues

Instituto de Física, Universidade Federal do Rio de Janeiro, Caixa Postal 68528, CEP 21941-972, Rio de Janeiro, Brazil

E-mail: mintz@if.ufrj.br, farina@if.ufrj.br, pamn@if.ufrj.br and robson@if.ufrj.br

Received 16 May 2006, in final form 20 July 2006
Published 18 August 2006
Online at stacks.iop.org/JPhysA/39/11325

Abstract

We consider a massless scalar field in 1+1 dimensions satisfying a Robin boundary condition (BC) at a non-relativistic moving boundary. We derive a Bogoliubov transformation between the input and output bosonic field operators, which allows us to calculate the spectral distribution of created particles. The cases of Dirichlet and Neumann BC may be obtained from our result as limiting cases. These two limits yield the same spectrum, which turns out to be an upper bound for the spectra derived for Robin BC. We show that the particle emission effect can be considerably reduced (with respect to the Dirichlet/Neumann case) by selecting a particular value for the oscillation frequency of the boundary position.

PACS numbers: 11.10.−z, 12.20.−m

1. Introduction

Moving bodies experience fundamental energy damping [1, 2] and decoherence [3] mechanisms due to the scattering of vacuum field fluctuations. The damping is accompanied by the emission of particles (photons in the case of the electromagnetic field) [4, 5], thus conserving the total energy of the body-plus-field system [6, 7]. This dynamical (or nonstationary) Casimir effect has been analysed for a variety of three-dimensional geometries, including parallel plane plates [8], cylindrical waveguides [9] and rectangular [10], cylindrical [11] and spherical cavities [12]. It also depends on the details of the coupling between the field and the body, which can usually be cast into the form of boundary conditions (BC) for the field.

Of particular theoretical relevance is the Robin BC, which continuously interpolates the Dirichlet and Neumann ones. For a scalar field, it reads

$$\frac{\partial \phi}{\partial n}(t, \mathbf{x}_0) = \frac{1}{\beta}\phi(t, \mathbf{x}_0), \tag{1}$$

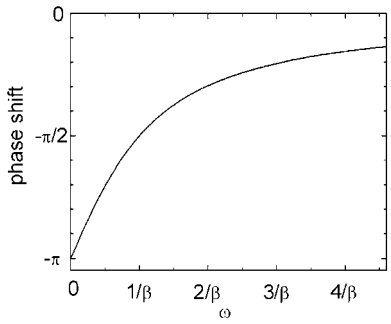

Figure 1. Phase shift φ between the reflected and incident waves as a function of ω for Robin BC at $x = 0$.

where $\mathbf{x}_0 \in \Sigma$, with Σ being the relevant boundary involved in the problem and $\partial/\partial n$ means normal derivative with respect to the boundary Σ. Though Robin BC can be considered for a massive scalar field in any dimensions, in this paper we shall be concerned with a massless scalar field in 1+1 dimensions satisfying this kind of condition in a non-relativistic moving boundary. Before attacking the problem of particle creation, a few comments about Robin BC are in order.

According to equation (1), Dirichlet and Neumann BC can be obtained as the limiting cases $\beta \to 0$ and $\beta \to \infty$, respectively. The positive parameter β represents a time scale (we take $c = 1$) associated with the time delay (or phase shift) characteristic of reflection at the Robin boundary. In fact, suppose an incident monochromatic wave propagating in the negative direction of the $\mathcal{OX}$ axis with wavenumber k and frequency ω reaches a Robin BC at $x = 0$. The solution for $x > 0$ is then given by the superposition of the incident wave with the reflected one obtained after the Robin BC is imposed, namely, $\phi(t, x) = A\,\mathrm{e}^{-\mathrm{i}(kx+\omega t)} + B\,\mathrm{e}^{\mathrm{i}(kx-\omega t)}$, where $\phi(t, 0) = \beta\frac{\partial\phi}{\partial x}(t, 0)$. Hence, it is straightforward to obtain the reflection coefficient at the boundary, $B/A =: r_R$, which is given by (we are using $c = 1$ so that $k = \omega$)

$$r_R = -\frac{1 + \mathrm{i}\beta\omega}{1 - \mathrm{i}\beta\omega} =: \mathrm{e}^{\mathrm{i}\varphi(\omega)}, \tag{2}$$

where $\varphi(\omega)$ is the phase shift between the reflected wave and the incident one shown in figure 1 as a function of ω.

Though the incident wave is totally reflected at the boundary, since $|r| = 1$, the existence of this phase shift gives origin to a time delay, which is discussed below. For this reason, Robin BC are also useful for phenomenological models which describe penetrable surfaces [13]. In order to see explicitly that these conditions, for some particular situations, simulate the plasma model for real metals, let us compute the reflection coefficient r_P using the plasma permittivity, $\varepsilon(\omega) = 1 - \omega_P^2/\omega^2$, where ω_P is the plasma frequency. In the limit $\omega \ll \omega_P$, it is not difficult to show that

$$r_P = -\mathrm{e}^{2\mathrm{i}\omega/\omega_P} + \mathcal{O}\left(\frac{\omega^2}{\omega_P^2}\right). \tag{3}$$

On the other hand, for $\omega \ll 1/\beta$, equation (2) allows us to write

$$r_R = -\mathrm{e}^{2\mathrm{i}\beta\omega} + \mathcal{O}(\beta^2\omega^2). \tag{4}$$

Comparing the last two equations, we conclude that for frequencies much smaller than the plasma frequency, $\omega \ll \omega_P$, the metallic boundary may be simulated by Robin BC, with

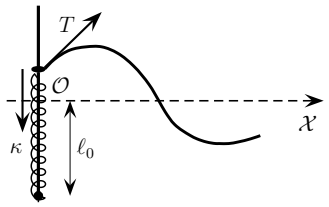

Figure 2. Elastic support at $x = 0$ giving rise to a Robin BC.

$1/\beta$ playing the role of the plasma frequency. Equivalently, β plays the role of the plasma wavelength λ_P, which is directly related to the penetration depth of the field into the metallic boundary.

In order to acquire further insight into the physical meaning of Robin BC, we discuss below a simple mechanical model where such conditions occur. Consider an infinite string under tension T tied to a massless ring that can slide without friction through a vertical rod, as indicated in figure 2. Suppose, also, that the ring is coupled to an ideal spring of elastic constant κ such that when the ring is at the origin the spring is neither compressed nor stretched. Since we are considering a massless ring, from Newton's second law and assuming small inclinations on the vibrating string ($|\partial y/\partial x| \ll 1$), we have

$$y(t, 0) = \frac{T}{\kappa}\frac{\partial y}{\partial x}(t, 0). \tag{5}$$

The above relation is precisely the definition of Robin BC, with T/κ playing the role of the parameter β. The fact that Robin BC simulates an elastic support at the boundary has been pointed out in the literature [14, 15]. Though the reflection at a fixed boundary with Robin BC is complete ($|r_R| = 1$), there is a time delay caused by the bulk/boundary dynamics. This may help in explaining qualitatively the existence of surface terms that appear in connection with Robin BC in quantum field theory [16–19].

A very detailed calculation was made by Romeo and Saharian concerning the static Casimir effect of a scalar field in 3+1 dimensions submitted to Robin BC at two parallel plates [19]. It is worth mentioning that Robin BC may give rise to restoring Casimir forces between the plates once parameters β at the plates are appropriately chosen.

In this paper, we shall consider a semi-infinite slab (extending from $-\infty$ to $x = \delta q(t)$) following a prescribed non-relativistic motion, with the Robin boundary at $\delta q(t)$. We have recently computed the dynamical Casimir force on a slab, which contains dissipative as well as dispersive components [15]. In this paper, we will analyse in detail the particle creation effect and compute the corresponding spectral distribution.

2. Input-output Bogoliubov transformation

In the instantaneously co-moving frame, the massless scalar field satisfies

$$\left.\frac{\partial \phi'}{\partial x'}\right|_{\text{bound}} = \left.\frac{1}{\beta}\phi'\right|_{\text{bound}}. \tag{6}$$

Neglecting terms of the order of $[\delta\dot{q}(t)]^2$, we find, in the laboratory frame,

$$\left[\frac{\partial}{\partial x} + \delta\dot{q}(t)\frac{\partial}{\partial t}\right]\phi(t, \delta q(t)) = \frac{1}{\beta}\phi(t, \delta q(t)). \tag{7}$$

We assume that the final position coincides with the initial one, which is taken at $x = 0$. Hence

$$\lim_{t\to\pm\infty} \delta q(t) = 0. \tag{8}$$

Jointly with the non-relativistic approximation, this condition implies that $\delta q(t)$ is much smaller than the wavelengths λ of the created particles. In fact, we will show that the frequencies of the particles are bounded by the mechanical frequencies $\omega_0 : \omega = 2\pi/\lambda \leqslant \omega_0$. Since $\omega_0 \delta q \sim \delta\dot{q} \ll 1$, we have $\delta q(t) \ll \lambda$.

Thus, we may analyse equation (7) by expanding up to first order in δq and its derivatives. This amounts to calculate the effect of the motion as a small perturbation [2]:

$$\phi(t, x) = \phi_0(t, x) + \delta\phi(t, x), \tag{9}$$

where the unperturbed field ϕ_0 corresponds to a solution with a static boundary at $x = 0$. The first-order field $\delta\phi$ then satisfies the following BC at $x = 0$:

$$\frac{\partial\delta\phi}{\partial x}(t, 0) - \frac{1}{\beta}\delta\phi(t, 0) = \delta q(t)\left[\frac{1}{\beta}\frac{\partial\phi_0}{\partial x}(t, 0) - \frac{\partial^2\phi_0}{\partial x^2}(t, 0)\right] - \delta\dot{q}(t)\frac{\partial\phi_0}{\partial t}(t, 0). \tag{10}$$

It is convenient to use the Fourier representation

$$\Phi(\omega, x) = \int \mathrm{d}t\, \mathrm{e}^{\mathrm{i}\omega t}\phi(t, x).$$

The unperturbed field satisfies the Robin BC at $x = 0$. Its normal mode expansion for $x > 0$ is given by

$$\Phi_0(\omega, x) = N(\omega)[\sin(\omega x) + \omega\beta\cos(\omega x)][\Theta(\omega)a(\omega) - \Theta(-\omega)a(-\omega)^\dagger], \tag{11}$$

with

$$N(\omega) = \sqrt{\frac{4\pi}{|\omega|(1 + \beta^2\omega^2)}}$$

and $\Theta(x)$ denoting Heaviside step function. The bosonic operators $a(\omega)$ and $a(\omega)^\dagger$ satisfy the commutation relation

$$[a(\omega), a(\omega')^\dagger] = 2\pi\delta(\omega - \omega'). \tag{12}$$

To solve equation (10) for $\delta\Phi(\omega, x)$ in terms of $\Phi_0(\omega, 0)$ (with $x > 0$), we use suitably defined Green functions, obeying the differential equation

$$\left(\frac{\partial^2}{\partial x^2} + \omega^2\right) G(\omega, x, x') = \delta(x - x'). \tag{13}$$

From Green's theorem, we find

$$\delta\Phi(\omega, x') = -\delta\Phi(\omega, 0)\frac{\partial}{\partial x}G(\omega, 0, x') + G(\omega, 0, x')\frac{\partial}{\partial x}\delta\Phi(\omega, 0). \tag{14}$$

This result is more easily combined with equation (10) if we select a solution $G_\mathrm{R}(\omega, x, x')$ of equation (13) satisfying the Robin BC at $x = 0$. With this Robin Green function, we immediately obtain the first-order field from equation (14) in terms of the BC satisfied by $\delta\Phi(\omega, x)$ as given by the Fourier transform of equation (10). Then, the complete field is written as

$$\Phi(\omega, x) = \Phi_0(\omega, x) + G_\mathrm{R}(\omega, 0, x)\left[\frac{\partial}{\partial x}\delta\Phi(\omega, 0) - \frac{\delta\Phi(\omega, 0)}{\beta}\right], \tag{15}$$

with

$$\frac{\partial}{\partial x}\delta\Phi(\omega,0)-\frac{\delta\Phi(\omega,0)}{\beta}=\frac{1}{\beta}\int\frac{\mathrm{d}\omega'}{2\pi}\left[\frac{\partial\Phi_0}{\partial x}(\omega,0)+\omega\omega'\Phi_0(\omega,0)\right]\delta Q(\omega-\omega'),\tag{16}$$

where $\delta Q(\omega)$ is the Fourier transform of $\delta q(t)$.

If we replace G_{R} in equation (15) by the retarded Robin Green function, given by

$$G_{\mathrm{R}}^{\mathrm{ret}}(\omega,0,x)=\frac{\beta}{1-\mathrm{i}\beta\omega}\,\mathrm{e}^{\mathrm{i}\omega x},\tag{17}$$

then the zeroth-order field $\Phi_0(\omega,x)$ corresponds to the input field $\Phi_{\mathrm{in}}(\omega,x)$, with

$$\phi_{\mathrm{in}}(t,x)=\lim_{t\to-\infty}\phi(t,x).$$

On the other hand, when taking the advanced Robin Green function, given by

$$G_{\mathrm{R}}^{\mathrm{adv}}(\omega,0,x)=\frac{\beta}{1+\mathrm{i}\beta\omega}\,\mathrm{e}^{-\mathrm{i}\omega x},\tag{18}$$

$\Phi_0(\omega,x)$ corresponds to the output field $\Phi_{\mathrm{out}}(\omega,x)$ ($\phi_{\mathrm{out}}(t,x)=\lim_{t\to\infty}\phi(t,x)$). By combining these two possibilities, we find the relation between the output and input fields:

$$\Phi_{\mathrm{out}}(\omega,x)=\Phi_{\mathrm{in}}(\omega,x)+\left[G_{\mathrm{R}}^{\mathrm{ret}}(\omega,0,x)-G_{\mathrm{R}}^{\mathrm{adv}}(\omega,0,x)\right]\left[\frac{\partial}{\partial x}\delta\Phi(\omega,0)-\frac{\delta\Phi(\omega,0)}{\beta}\right].\tag{19}$$

The final result is obtained by inserting equations (16) (with Φ_0 replaced by Φ_{in} since we neglect terms of second order), (17) and (18) into the rhs of equation (19). Further physical insight is gained if we write the input–output relation in terms of the annihilation operators a_{in}, a_{out} and their Hermitian conjugates, by combining equations (11) and (19). The resulting input–output relation has the form of a Bogoliubov transformation:

$$\begin{aligned}a_{\mathrm{out}}(\omega)=a_{\mathrm{in}}(\omega)+\frac{2\mathrm{i}\sqrt{\omega}}{\sqrt{1+\beta^2\omega^2}}\int\frac{\mathrm{d}\omega'}{2\pi}\frac{1+\beta^2\omega\omega'}{\sqrt{1+\beta^2\omega'^2}}\sqrt{|\omega'|}\\ \times\left[\theta(\omega')a_{\mathrm{in}}(\omega')-\theta(-\omega')a_{\mathrm{in}}(-\omega')^{\dagger}\right]\delta Q(\omega-\omega').\end{aligned}\tag{20}$$

Since the output annihilation operator is contaminated by the input creation operator, the input vacuum state $|0_{\mathrm{in}}\rangle$ is not a vacuum state with respect to the output operators. In the next section, we compute the resulting particle creation effect.

3. Frequency spectrum

The number of particles created with frequencies between ω and $\omega+\mathrm{d}\omega$ ($\omega\geqslant 0$) is

$$\frac{\mathrm{d}N}{\mathrm{d}\omega}(\omega)\,\mathrm{d}\omega=\langle 0_{\mathrm{in}}|a_{\mathrm{out}}(\omega)^{\dagger}a_{\mathrm{out}}(\omega)|0_{\mathrm{in}}\rangle\frac{\mathrm{d}\omega}{2\pi}.\tag{21}$$

The spectrum is obtained by inserting equation (20) into (21):

$$\frac{\mathrm{d}N}{\mathrm{d}\omega}(\omega)=\frac{2\omega}{\pi(1+\beta^2\omega^2)}\int_0^{\infty}\frac{\mathrm{d}\omega'}{2\pi}\frac{\omega'[1-\beta^2\omega\omega']^2}{1+\beta^2\omega'^2}|\delta Q(\omega+\omega')|^2.\tag{22}$$

To single out the effect of a given Fourier component of the motion, we take

$$\delta q(t)=\delta q_0\cos(\omega_0 t)\,\mathrm{e}^{-|t|/T},$$

with $\omega_0 T\gg 1$. In this case, $\delta Q(\omega)$ corresponds to two very narrow peaks around $\omega=\pm\omega_0$, so that we may take the approximation

$$|\delta Q(\omega)|^2\approx\frac{\pi}{2}\delta q_0^2 T\left[\delta(\omega-\omega_0)+\delta(\omega+\omega_0)\right].\tag{23}$$

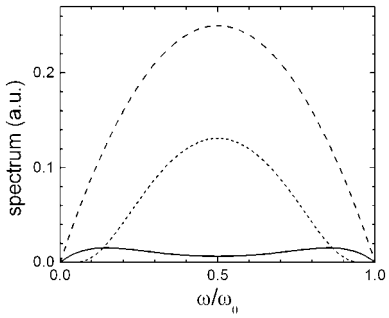

Figure 3. Spectral distribution of the emitted particles $\mathrm{d}N/\mathrm{d}\omega$. For the horizontal scale, we divide the frequencies by the mechanical frequency ω_0. Dashed line: $\beta = 0$ (Dirichlet case), solid line: $\beta\omega_0 = 1.7$, dotted line $\beta\omega_0 = 5$.

Inserting this equation into (22), we find

$$\frac{\mathrm{d}N}{\mathrm{d}\omega}(\omega) = \frac{\delta q_0^2 T}{2\pi}\omega(\omega_0-\omega)\frac{[1-\beta^2\omega(\omega_0-\omega)]^2}{(1+\beta^2\omega^2)[1+\beta^2(\omega_0-\omega)^2]}\Theta(\omega_0-\omega). \tag{24}$$

Note that the spectrum vanishes for $\omega > \omega_0$: no particle is created with frequency larger than the mechanical frequency. Field modes at higher frequencies are not excited by the motion, which is slow in the time scale corresponding to such frequencies (quasi-static regime). This important property confirms the consistency of our perturbation approach, with its expansion in $\delta q/\lambda$.

A second important general property of the spectrum given by equation (24) is the symmetry around $\omega = \omega_0/2$: the spectrum is invariant under the replacement $\omega \to \omega_0 - \omega$. This is a signature that the particles are created in pairs, with frequencies such that their sum equals ω_0. Hence, for each particle created at frequency ω, there is a 'twin' particle created at frequency $\omega_0 - \omega$.

Since Robin BC interpolate Dirichlet and Neumann ones, we may derive the spectra for these two cases by taking appropriate limits of equation (24). For Dirichlet BC, we find

$$\left.\frac{\mathrm{d}N_{(D)}}{\mathrm{d}\omega}(\omega)\right|_{(D)} = \lim_{\beta\to 0}\frac{\mathrm{d}N}{\mathrm{d}\omega}(\omega) = \frac{(\delta q_0)^2 T}{2\pi}\omega(\omega_0-\omega)\Theta(\omega_0-\omega), \tag{25}$$

in agreement with [6]. For the Neumann BC ($\beta \to \infty$), we find the *same spectrum*, confirming the equivalence between Dirichlet and Neumann in the context of the dynamical Casimir effect in 1+1 dimensions [20].

For intermediate values of β, the spectrum is always *smaller* than in the Dirichlet case for all values of ω. In fact, we may write the result of equation (24) as

$$\frac{\mathrm{d}N}{\mathrm{d}\omega}(\omega) = \eta\frac{\mathrm{d}N_{(D)}}{\mathrm{d}\omega}(\omega), \tag{26}$$

where the *reduction factor* $\eta \leqslant 1$ is a function of $\beta\omega_0$ and ω/ω_0. The reduction may be more severe near $\omega = \omega_0/2$, which is the spectrum maximum in the Dirichlet case, for some values of $\beta\omega_0$. Hence, the Robin spectrum may develop global maxima near $\omega = 0$ and $\omega = \omega_0$, as in the example shown in figure 3 (solid line), with $\beta\omega_0 = 1.7$. In this figure, we also plot the Dirichlet/Neumann spectrum (dashed line) and the Robin spectrum for $\beta\omega_0 = 5$ (dotted line). As discussed above, all curves are symmetric with respect to $\omega = \omega_0/2$.

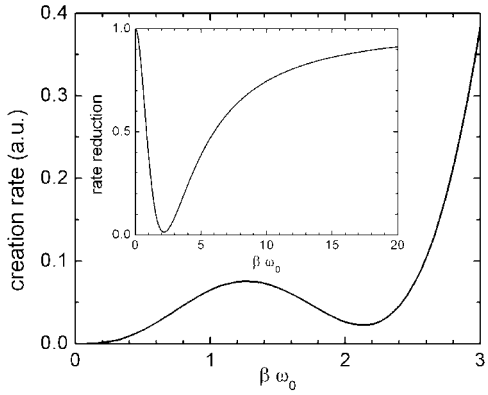

Figure 4. Total particle creation rate as a function of mechanical frequency (in units of $1/\beta$). Inset: ratio between creation rates for Robin and Dirichlet BC.

The areas below the curves shown in figure 3 correspond to the total number of created particles. The figure already indicates that this number, to be discussed in the next section, may be considerably reduced (with respect to the Dirichlet case) for intermediate values of β.

4. Particle creation rate

The total number of created particles is given by

$$N = \int_0^{\omega_0} \frac{\mathrm{d}N}{\mathrm{d}\omega}(\omega)\,\mathrm{d}\omega = \frac{\delta q_0^2 T}{2\pi}\omega_0^3 F(\beta\omega_0), \tag{27}$$

with

$$F(\xi) = \frac{\xi[4\xi + \xi^3 + 12\arctan(\xi)] - 6(2+\xi^2)\ln(1+\xi^2)}{6\xi^2(4+\xi^2)}. \tag{28}$$

As expected for an open geometry (with a continuum of field modes), N is proportional to time T, so that the particle creation *rate* $R \equiv N/T$ is the physically meaningful quantity. For the Dirichlet case, we take $F(\xi \to 0) = 1/6$, and then

$$R_{(D)} = \frac{\delta q_0^2 \omega_0^3}{12\pi}. \tag{29}$$

For the Neumann case, we find the same result for the creation rate, since the spectrum is the same. Note that the rate *increases* with ω_0 according to equation (29) and vanishes (as required) in the static limit $\omega_0 = 0$. This could have been anticipated since the particle creation is an effect of changing the BC nonadiabatically. However, for Robin BC the rate is not a monotonic function of ω_0. In figure 4, we plot the rate R as a function of $\beta\omega_0$ (for a fixed β). R decreases as ω_0 varies from $1.3/\beta$ to the local minimum at $2.1/\beta$.

In the inset of figure 4, we plot the ratio $R/R_{(D)} = 6F(\beta\omega_0) \leqslant 1$ as a function of $\beta\omega_0$. This ratio represents the reduction of the Dirichlet creation rate for a finite β. It only depends on the dimensionless variable $\beta\omega_0$ and goes asymptotically to one for $\beta\omega_0 \gg 1$, since the Neumann BC yields the same rate as the Dirichlet case. The reduction is maximum at $\beta\omega_0 = 2.2$. At this point, the creation rate is reduced to 1.3% of the Dirichlet value[1].

[1] When plotting the creation rate itself, the effect seems to be less impressive because the Dirichlet rate increases with ω_0.

Since the relevant field frequencies are bounded by the inequality $\omega \leqslant \omega_0$, these results may be interpreted with the help of figure 1, which shows the variation of the phase φ acquired in the reflection by the Robin boundary as a function of ω. When $\omega_0 \ll 1/\beta$, all the relevant field modes are reflected as in the Dirichlet case ($\varphi \approx -\pi$) and the creation rate is close to the Dirichlet value, as expected. As ω_0 approaches $1/\beta$, most field modes probe the non-trivial sector shown in figure 1, with phase factors very different from $-\pi$. This mimics the phase resulting from penetration in metals with finite conductivity, as for instance in the theoretical framework of the plasma model described in the introduction. Hence, it is not surprising that the dynamical Casimir effect is reduced, a result which is analogous to the reduction of the static Casimir effect when finite conductivity is considered. In particular, when ω_0 is close to $2/\beta$, the centre of the spectrum (see figure 1) is close to $\omega = 1/\beta$, where the phase has a maximum deviation from the Dirichlet/Neumann values. This explains the stronger reduction near the centre of the spectrum shown by the solid line in figure 3. For instance, for $\beta\omega_0 = 2$, $\mathrm{d}N/\mathrm{d}\omega = 0$ at $\omega = \omega_0/2 = 1/\beta$.

On the other hand, when $\omega_0 \gg 1/\beta$, the non-trivial sector of the spectrum is a tiny fraction of the relevant range $0 \leqslant \omega \leqslant \omega_0$. As a consequence, most frequencies are reflected as in the Neumann case ($\varphi = 0$) and the creation rate approaches the common value for Dirichlet/Neumann BC.

We may also calculate the radiated energy from these results. Thanks to the symmetry of the spectrum around $\omega = \omega_0/2$, we have

$$E = \int_0^{\omega_0} \frac{\mathrm{d}N}{\mathrm{d}\omega}(\omega)\hbar\omega\,\mathrm{d}\omega = \frac{\hbar\omega_0}{2}N. \tag{30}$$

Combining with equation (27), we find

$$E = \delta q_0^2 T\hbar\omega_0^4 F(\beta\omega_0)/(4\pi). \tag{31}$$

This expression can be directly compared with the result for the Casimir force we have recently reported [15]. The force is written (in the Fourier domain) as $\mathcal{F}(\omega) = \chi(\omega)\delta Q(\omega)$ and its work on the slab is given in terms of the imaginary part of the susceptibility function $\chi(\omega)$:

$$W = -\frac{1}{\pi}\int_0^{\infty} \mathrm{d}\omega\,\omega\,\mathrm{Im}\,\chi(\omega)|\delta Q(\omega)|^2. \tag{32}$$

For the quasi-sinusoidal motion considered here, we find, using equation (23),

$$W = -\delta q_0^2 T\omega_0\,\mathrm{Im}\,\chi(\omega_0)/2. \tag{33}$$

The result for $\mathrm{Im}\,\chi(\omega_0)$ derived in [15] can be cast in the form[2] $\mathrm{Im}\chi(\omega_0) = \hbar\omega_0^3 F(\beta\omega_0)/(2\pi)$. Then, the comparison of equations (31) and (33) yield $E = -W$, so that the total radiated energy coincides with the negative of the work done on the slab by the Casimir force, as expected from energy conservation.

5. Conclusion

Dirichlet ($\beta \to 0$) and Neumann BC ($\beta \to \infty$) yield the same result for the spectrum of the created particles. With the Robin BC, we are able to interpolate continuously between

[2] In [15], a narrow plate is considered, rather than a slab. The two sides of the plate provide identical (and independent) contributions to the force, because Robin BC do not allow for any coupling between the fields in each side. In fact, the two sides correspond to independent field operators and Hilbert spaces. To compare with the present situation, we divide the result of [15] by 2.

these two cases. For intermediate values of β, the spectrum is always smaller than the Dirichlet/Neumann case, for all values of frequency.

In the range $1.2 < \beta\omega_0 < 2.4$ the spectrum develops lateral peaks higher than the value at $\omega = \omega_0/2$. This is also approximately the range in which the total creation rate (surprisingly) decreases with ω_0. This rate is reduced by up to 1.3% of the Dirichlet/Neumann value, if the mechanical frequency is selected at $\omega_0 = 2.2/\beta$. In other words, the coupling with the vacuum field state is considerably reduced if the slab oscillates at a frequency close to this value.

When considering the electromagnetic field and a plane mirror moving along its normal direction, the BC in the ideal case of *perfect reflectors* may be decomposed into Dirichlet and Neumann BC for each orthogonal polarization [21]. In 3+1 dimensions, the effect with Neumann BC is considerably larger than with Dirichlet BC and it would be interesting to investigate the continuous transition between these two limiting cases.

Reflection by real metallic plates involves non-trivial frequency-dependent phase factors as in the case of Robin BC. The results of the present paper indicate that finite conductivity might yield a reduction of the magnitude of the dynamical Casimir effect.

Acknowledgments

This work was supported by the Brazilian agencies CNPq and FAPERJ. PAMN also acknowledges Institutos do Milênio de Informação Quântica e Nanociências for partial financial support.

References

[1] Fulling S A and Davies P C W 1976 *Proc. R. Soc. London* A **348** 393
Jaekel M T and Reynaud S 1992 *Quant. Opt.* **4** 39
Maia Neto P A and Reynaud S 1993 *Phys. Rev.* A **47** 1639
[2] Ford L H and Vilenkin A 1982 *Phys. Rev.* D **25** 2569
[3] Dalvit D A R and Maia Neto P A 2000 *Phys. Rev. Lett.* **84** 798
[4] Moore G T 1970 *Math. Phys.* **11** 2679
[5] Special Issue on the Nonstationary Casimir effect quantum systems with moving boundaries 2005 *J. Opt. B: Quantum Semiclass. Opt.* **7** S3
[6] Lambrecht A, Jaekel M-T and Reynaud S 1996 *Phys. Rev. Lett.* **77** 615
[7] Maia Neto P A and Machado L A S 1996 *Phys. Rev.* A **54** 3420
[8] Mundarain D F and Maia Neto P A 1998 *Phys. Rev.* A **57** 1379
[9] Maia Neto P A 2005 *J. Opt. B: Quantum Semiclass. Opt.* **7** S86
[10] Dodonov V V and Klimov A B 1996 *Phys. Rev.* A **53** 2664
Crocce M, Dalvit D A R and Mazzitelli F D 2001 *Phys. Rev.* A **64** 013808
Schaller G, Schützhold R, Plunien G and Soff G 2002 *Phys. Rev.* A **66** 023812
[11] Crocce M, Dalvit D A R, Lombardo F C and Mazzitelli F D 2005 *J. Opt. B: Quantum Semiclass. Opt.* **7** S32
[12] Eberlein C 1996 *Phys. Rev. Lett.* **76** 3842
[13] Mostepanenko V M and Trunov N N 1985 *Sov. J. Nucl. Phys.* **45** 818
[14] Chen G and Zhou J 1993 *Vibration and Damping in Distributed Systems* vol I (Boca Raton, FL: CRC) p 15
[15] Mintz B, Farina C, Maia Neto P A and Rodrigues R 2006 *J. Phys. A: Math. Gen.* **39** 6559
[16] de Albuquerque L C and Cavalcanti R M 2004 *J. Phys. A: Math. Gen.* **37** 7039
[17] Fulling S A 2003 *J. Phys. A: Math. Gen.* **36** 6857
[18] Kennedy G, Critchley R and Dowker J S 1980 *Ann. Phys., NY* **125** 346
[19] Romeo A and Saharian A A 2002 *J. Phys. A: Math. Gen.* **35** 1297
[20] Alves D T, Farina C and Maia Neto P A 2003 *J. Phys. A: Math. Gen.* **36** 1133
[21] Maia Neto P A 1994 *J. Phys. A: Math. Gen.* **27** 2167